22. T. Kataoka, S. Kondo, M. Nishi, M. Kodaira, T. Honjo, *Nucleic Acids Res.* 12, 5995 (1984).
23. T. Blackwell and F. Alt, *Cell* 37, 105 (1984).
24. D. Wood and C. Colecough, *Proc. Nat. Acad. Sci. U.S.A.* 81, 4756 (1984).
25. S. Gerondakis, S. Cory, J. Adams, *Cell* 36, 973 (1984).
26. L. Corcoran, S. Cory, J. Adams, *ibid.* 40, 71 (1985).
27. T. Nikaido, Y. Yamawaki-Kataoka, T. Honjo, *J. Biol. Chem.* 257, 7322 (1982).
28. R. Aguilera, T. Hope, H. Sakano, *EMBO J.* 4, 3689 (1985).
29. S. Lewis, A. Gifford, D. Baltimore, *Science* 228, 677 (1985).
30. Supported by NIH grant AI-18790, and ACS grant IM-366 and a predoctoral fellowship from NSF (R.J.A.). We thank Dr. Anthony Otsuka for critical reading of the manuscript and Dr. Olli Vainio for advice on the preparation of chick embryo bursa.

7 June 1985; accepted 5 December 1985

Atrial Natriuretic Peptide Elevation in Congestive Heart Failure in the Human

J. C. BURNETT, JR.,* P. C. KAO, D. C. HU, D. W. HESER, D. HEUBLEIN, J. P. GRANGER, T. J. OPGENORTH, G. S. REEDER

A sensitive radioimmunoassay for atrial natriuretic peptide was used to examine the relation between circulating atrial natriuretic peptide and cardiac filling pressure in normal human subjects, in patients with cardiovascular disease and normal cardiac filling pressure, and in patients with cardiovascular disease and elevated cardiac filling pressure with and without congestive heart failure. The present studies establish a normal range for atrial natriuretic peptide in normal human subjects. These studies also establish that elevated cardiac filling pressure is associated with increased circulating concentrations of atrial natriuretic peptide and that congestive heart failure is not characterized by a deficiency in atrial natriuretic peptide, but with its elevation.

RECENT INVESTIGATIONS HAVE documented the existence of specific secretory granules that have vasoactive properties (*1–6*). Studies from various laboratories have established that administration of synthetic atrial natriuretic peptide (ANP) in animals results in natriuresis, decrease in arterial pressure, and inhibition of the renin-angiotensin-aldosterone system, supporting a role for the atrial peptide system in cardiovascular volume regulation (*7, 8*). Thrasher and colleagues have reported that acute increases in cardiac filling pressures in conscious dogs result in enhanced release of circulating ANP, suggesting that cardiac volume or pressure or both may be important in determining the release of ANP (*9*). Chimoskey and co-workers have reported that hamsters with familial cardiomyopathy and congestive heart failure are deficient in ANP as determined by bioassay (*10*). These investigators speculated that failure to produce sufficient ANP by the degenerating hearts of cardiomyopathic hamsters contributes to the retention of sodium and water with formation of edema. No studies have been performed to define the relation in humans between circulating levels of ANP and cardiac filling pressures. Further, no studies have established whether the syndrome of congestive heart failure is characterized by a deficiency in ANP.

We determined circulating concentrations of ANP in normal human volunteers with no history of cardiovascular disease (group 1, n = 14), patients with cardiovascular disease but normal cardiac filling pressures (group 2, n = 11), patients with cardiovascular disease and markedly elevated cardiac filling pressures but without congestive heart failure (group 3, n = 6), and patients with cardiovascular disease, markedly elevated cardiac filling pressures, and congestive heart failure (group 4, n = 6).

We determined the circulating concentrations of ANP with a newly developed, sensitive, nonequilibrium radioimmunoassay for human α-ANP. The synthetic peptide of human α-ANP (Peninsula Laboratory) was used to prepare standard and tracer. We labeled human α-ANP with $Na^{125}I$ by the Iodogen procedure. The crude, labeled peptide was purified first on a Bio-Rad P-2 column and then by high-performance liquid chromatography (HPLC) on a C_{18} column (Fig. 1A). For the radioimmunoassay, we first incubated rabbit antiserum to human α-ANP (RAS-8798, Peninsula Laboratory) in the presence of standard or sample for 24 hours and then added the labeled ANP for an additional 16 hours of incubation, both at 4°C. Free and bound fractions

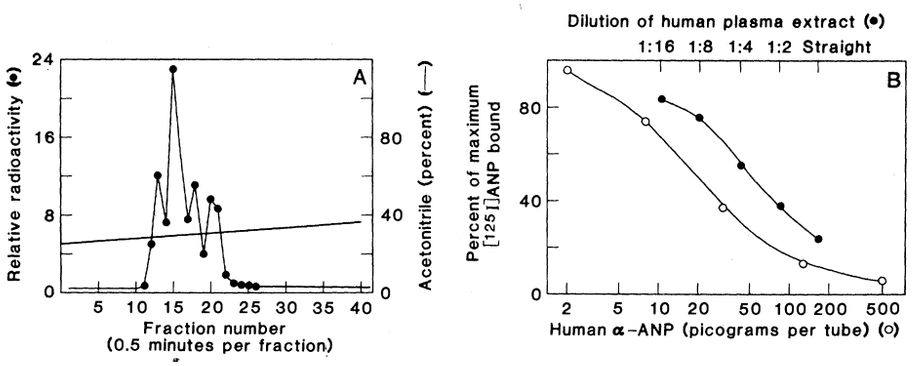

Fig. 1. Radioimmunoassay for human α-ANP. Synthetic human α-ANP (2 μg in 20 μl of 0.5*M* sodium phosphate buffer, *p*H 7.4) was iodinated with 2 mCi of $Na^{125}I$ (Amersham) by 2.5 μg of Iodogen (Pierce Chemical), which had been dissolved in dichloromethane and evaporated to dryness in a test tube. The reaction mixture was first purified on a Bio-Rad P-2 column (0.8 by 15 cm) eluted with 0.1*M* acetic acid containing 0.1 percent bovine serum albumin (BSA). Then it was further purified on a μBondapak C_{18} column with a linear gradient of 25 to 35 percent acetonitrite in a solution of 0.1 percent trifluoroacetic acid. Four peaks showing radioactivity were obtained (A), all of which had equivalent immunobinding ability with rabbit antiserum to human α-ANP. The second peak was used for the radioimmunoassay. The purified, labeled human α-ANP was diluted in assay buffer (0.1*M* sodium phosphate, 0.05*M* NaCl, 0.1 percent BSA, 0.1 percent Triton X-100, and 0.01 percent sodium azide) to a concentration of 10,000 counts per minute per 100 μl as total count per tube. Rabbit antiserum to human α-ANP was also diluted in assay buffer to a concentration such that 100 μl of the solution would bind 35 percent of the total count in the absence of standard. The standard curve was constructed by serial dilution of synthetic human α-ANP from 500 pg to 1.8 pg per 100 μl. The antibody and standard were incubated together for 24 hours at 4°C, after which labeled human α-ANP was added to incubate for an additional 16 hours, both at 4°C. Free and bound fractions were separated by precipitation with the second antiserum in the presence of 2 percent polyethylene glycol 8000. The mixtures were incubated for 30 minutes at 4°C and then centrifuged. The supernatants, or free fractions, were aspirated and discarded; the precipitates, or bound fractions, were counted in a gamma counter, and standard curves were calculated (open circles in B). A curve constructed from results of a serial dilution of a human plasma extract with assay buffer showed parallelism to the standard curve (closed circles in B).

Departments of Internal Medicine and Laboratory Medicine, Mayo Medical School, Rochester, MN 55905.

*To whom correspondence should be addressed.

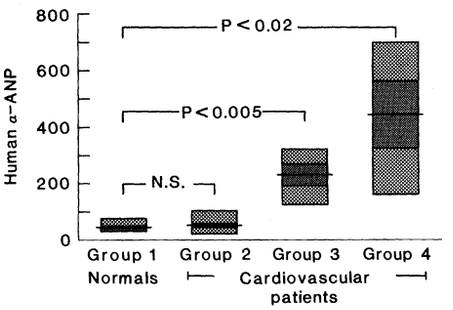

Fig. 2. Plasma concentrations of α-ANP (in picograms per milliliter) in normal subjects and cardiovascular patients. Samples of separated plasma (1 ml) were applied to a 500-mg C_{18} cartridge, which was washed with 4 ml of methanol and then with 4 ml of water. After the plasma was applied, the cartridge was washed with 2 ml of normal saline, 6 ml of water, and 1 ml of methanol. α-ANP was eluted from the cartridge with 2 ml of 75 percent methanol in 1 percent trifluoroacetic acid. The eluate was evaporated to dryness and reconstituted in assay buffer for radioimmunoassay. The complete vertical bar indicates the range of ANP concentrations in the plasma. Middle horizontal bars indicate means, and upper and lower horizontal bars indicate standard errors. The data were analyzed by the Behrens-Fisher *t* test. N.S., not significant.

of human α-ANP were separated by precipitation with goat antiserum to rabbit immunoglobulin G (second antibody); the incubation period with second antibody was 30 minutes. The sensitivity of this assay is 3 pg ml^{-1}. Total binding is 35 percent, and the 50 percent displacement point on a standard curve is 28 pg (Fig. 1B).

Blood was drawn from patients into tubes containing chilled potassium EDTA and was immediately placed on ice until being centrifuged at 4°C. Plasma was separated and frozen at −20°C until assay. Before the radioimmunoassay, we used C_{18} cartridges (Bond Elut) to extract ANP from the plasma and to remove impurities. The eluted ANP was dried and reconstituted for the radioimmunoassay. The recovery of the extraction procedure was 81 ± 2.0 percent (mean standard error of the mean) as determined by addition of synthetic ANP to plasma. Interassay and intraassay variations were 9 and 6 percent, respectively (Fig. 1B).

Plasma samples were obtained from normal human volunteers (group 1) and from patients undergoing consecutive diagnostic right or left heart catheterization. Cardiovascular medications including β-antagonists, calcium antagonists, diuretics, vasodilators, and cardiac glycosides were withheld from the subjects on the day of cardiac catheterization. Congestive heart failure was defined on the basis of signs and symptoms characteristic of the syndrome (peripheral edema, hepatomegaly, orthopnea, and paroxysmal nocturnal dyspnea). Normal cardiac filling pressure was defined as pulmonary capillary wedge pressure or left ventricular end diastolic pressure equal to or less than 10 mmHg. In group 1 (normal human volunteers), ANP concentrations ranged from 31 to 76 pg ml^{-1}, with a mean of 44.6 ± 3.7. Concentrations in group 2 were not significantly different from those in normal volunteers (Table 1 and Fig. 2). Concentrations of ANP were significantly elevated in group 3 compared to group 1 ($P < 0.005$) (Table 1). In group 4, ANP concentrations were significantly increased above those in group 1 ($P < 0.02$).

We have shown that marked elevation of cardiac filling pressure associated with cardiovascular disease with or without the syndrome of congestive heart failure is associated with significant elevation of circulating ANP concentrations compared with values for normal volunteers and patients with cardiovascular disease but normal cardiac filling pressures. Our studies extend the animal studies of Thrasher and colleagues and demonstrate an important relation between cardiac filling pressure and circulating concentrations of ANP. This implies that cardiac filling pressure may determine the release of ANP (*9*).

The observations also provide insight into the pathophysiology of congestive heart failure. In patients with congestive heart failure, as manifested by marked elevation of cardiac filling pressure, peripheral edema, and pulmonary congestion, concentrations of ANP were increased. Thus, the sodium retention and edema formation characteristic of congestive heart failure occurs despite increased circulating ANP levels. Indeed, the patients with the highest concentrations of circulating ANP had symptoms of biventricular failure, which is consistent with recent animal studies that have reported an attenuated natriuretic response to exogenously administered synthetic ANP in acute experimental heart failure (*11, 12*). Thus our study establishes that, in human subjects, congestive heart failure reflects not an ANP deficiency state but rather a compensatory increase in peptide release.

Table 1. Individual patient profiles, showing hemodynamic data and concentrations of atrial natriuretic peptide (ANP, in picograms per milliliter of plasma). Other abbreviations: MAP, mean arterial pressure; HR, heart rate (in beats per minute); CFP, cardiac filling pressure; CAD, coronary artery disease; ACP, atypical chest pain; NCA, normal coronary arteries; EH, essential hypertension; RC, restrictive cardiomyopathy; AS, aortic stenosis; IC, ischemic cardiomyopathy; IDC, idiopathic dilated cardiomyopathy. Values are expressed as means ± standard errors of the means.

Patient	Age (years)	Sex	MAP (mmHg)	HR	CFP (mmHg)	ANP	Clinical diagnosis
				Group 2			
1	69	M	98	62	8	104	CAD
2	64	F	58	46	10	54	CAD
3	33	M	76	70	7	33	CAD
4	48	M	93	55	10	73	CAD
5	31	M	113	98	6	47	ACP, NCA
6	47	M	107	65	10	57	EH, CAD
7	60	M	89	70	8	63	CAD
8	41	M	105	76	9	37	CAD
9	43	M	94	65	7	22	CAD
10	65	M	65	90	5	33	CAD
11	49	F	79	63	7	47	CAD
Mean			89 ± 5	67 ± 4	7.9 ± 0.5	51.8 ± 6.9	
				Group 3			
12	74	M	107	57	25	316	CAD
13	54	M	83	46	31	126	EH, CAD
14	68	M	108	73	30	314	EH, CAD
15	73	M	92	63	28	323	CAD
16	75	M	97	90	29	140	CAD
17	82	M	109	73	22	173	CAD
Mean			99 ± 4	67 ± 6	27.5 ± 1.3*	232.0 ± 38.8*	
				Group 4			
18	76	M	105	44	34	700	RC, CAD, EH
19	55	M	83	62	21	215	AS
20	68	F	68	68	23	746	IC
21	74	M	88	66	29	164	IC
22	66	F	94	67	33	162	IC
23	29	M	84	72	32	685	IDC
Mean			87 ± 5	64 ± 3	26.8 ± 2.3*	445.3 ± 119.3*	

*$P < 0.005$ (Behrens-Fisher *t* test) calculated for the values in group 3 or 4 against values in group 2.

REFERENCES AND NOTES

1. A. J. DeBold, *Life Sci.* **28**, 89 (1981).
2. T. H. Flynn, M. DeBold, A. DeBold, *Biochem. Biophys. Res. Commun.* **117**, 859 (1983).
3. S. A. Atlas, *Nature (London)* **309**, 717 (1984).
4. M. G. Currie *et al.*, *Science* **223**, 67 (1984).
5. K. S. Misono, *Biochem. Biophys. Res. Commun.* **119**, 524 (1984).
6. N. G. Seldah, *Proc. Natl. Acad. Sci. U.S.A.* **81**, 2640 (1984).
7. J. C. Burnett, Jr., J. P. Granger, T. J. Opgenorth, *Am. J. Physiol.* **247**, F863 (1984).
8. T. Maack, *Am. J. Med.* **77**, 1069 (1984).
9. T. N. Thrasher *et al.*, *Fed. Proc. Fed. Am. Soc. Exp. Biol.* **44**, 7711 (1985).
10. J. E. Chimoskey, W. S. Spielman, M. A. Brandt, S. R. Heidemann, *Science* **223**, 820 (1984).
11. R. H. Freeman, J. O. Davis, R. Vari, *Am. J. Physiol.* **248**, R495 (1985).
12. T. A. Scriven, J. C. Burnett, Jr., *Circulation* **72**, 892 (1985).
13. Supported by American Heart Association grant-in-aid 83-964 and by the Hearst, Rappaport, and Mayo Foundations.

8 July 1985; accepted 21 November 1985

Expression and Modulation of Voltage-Gated Calcium Channels After RNA Injection in *Xenopus* Oocytes

NATHAN DASCAL, TERRY P. SNUTCH, HERMANN LÜBBERT, NORMAN DAVIDSON, HENRY A. LESTER*

Calcium ions flow into cells through several distinct classes of voltage-dependent calcium-selective channels. Such fluxes play important roles in electrical signaling at the cell membrane and in chemical signaling within cells. Further information about calcium channels was obtained by injecting RNA isolated from rat brain, heart, and skeletal muscle into *Xenopus* oocytes. Macroscopic currents through voltage-operated calcium channels were resolved when the endogenous calcium-dependent chloride current was blocked by replacing external calcium with barium and chloride with methanesulfonate. The resulting barium current was insensitive to tetrodotoxin but was completely blocked by cadmium or cobalt. With both heart and brain RNA at least two distinct types of calcium ion conductance were found, distinguishable by their time course and inactivation properties. In oocytes injected with heart RNA, the slowly inactivating component was selectively blocked by the calcium-channel antagonist nifedipine. Barium ion currents induced by heart RNA were modulated by isoproterenol, cyclic adenosine monophosphate, and acetylcholine.

ELECTRICALLY EXCITABLE Ca^{2+} CHANNELS are widespread in nerve, muscle, and several other eukaryotic cell types (*1*). These channels regulate the flow of Ca^{2+} into the cell, where it functions in the contraction of muscle, the release of neurotransmitters and hormones, and the activation of other channels. Several types of Ca^{2+} channels can be distinguished on the basis of the waveform of the currents, voltage- and Ca^{2+}-dependent inactivation, single-channel conductance, and sensitivity to blocking agents (*2*). Ca^{2+} channels can be modulated by neurotransmitters acting through intracellular second messengers. A multisubunit protein complex, presumed to be the Ca^{2+} channel, has been enriched from skeletal muscle by biochemical fractionations in which the binding of dihydropyridine Ca^{2+}-channel antagonists is used as an assay (*3*).

It would be desirable to characterize the individual Ca^{2+} channel types in a similar membrane environment that also permits the introduction of modulatory elements. *Xenopus* oocytes provide an excellent preparation for such studies because (i) they translate and process exogenous messenger RNA (mRNA) efficiently (*4*); (ii) they are amenable to modern electrophysiological measurements, including voltage- and patch-clamp methods; and (iii) several intracellular messenger systems have been identified and characterized (*5*).

To characterize Ca^{2+} currents in oocytes injected with mRNA isolated from electrically excitable tissues, we first identified the endogenous Ca^{2+} currents in uninjected oocytes. The oocytes were tested with a voltage-clamp circuit that used two intracellular microelectrodes. Stepping the voltage from a holding potential of −100 to 0 mV in a normal solution containing 1.8 m*M* Ca^{2+} resulted in both a transient outward current of amplitude 20 to 50 nA lasting for 0.5 to 1 second and a slowly activating K^+ current (Fig. 1). Previous studies have shown that the transient current is a chloride current, $I_{Cl(Ca)}$, evoked by the entry of Ca^{2+} through voltage-dependent Ca^{2+} channels; however, the underlying Ca^{2+} current has not been detected (*6*). To resolve currents through the putative Ca^{2+} channels, we found it necessary to replace the Ca^{2+} with Ba^{2+} (40 m*M*) and to replace the Cl^- with methanesulfonate (legend to Fig. 1). In this solution, both the leak and the slow outward currents were reduced, $I_{Cl(Ca)}$ disappeared, and a transient inward current (decay time constant, ~0.5 second) was observed (Fig. 1, C and D). This conductance was smaller than most conductances observed in *Xenopus* oocytes; the net peak amplitude (after subtracting the leak current) was usually less than 10 nA, and the currents of Fig. 1, C and D, were the largest recorded in more than 25 oocytes. This current also appeared in a Cl^--free solution with high concentrations of Ba^{2+} and *N*-methyl-D-glucamine substituted for Na^+; it was therefore not a Na^+ current. It was, however, completely inhibited by 0.5 to 1 m*M* Cd^{2+} or by 2 m*M* Co^{2+}. The current was activated at voltages more positive than −30 mV and had a bell-shaped current-voltage curve that peaked at about 10 mV (Fig. 1E). Taken together, these results suggest that the transient inward current was a Ba^{2+} current (I_{Ba}) through a Ca^{2+} channel. Like $I_{(Cl(Ca)}$ (*6*) I_{Ba} was almost fully inactivated by holding potentials more positive than −40 mV (Fig. 1F).

Xenopus oocytes were injected with either total RNA or polyadenylated [poly(A)$^+$] RNA isolated from rat liver, skeletal muscle, heart, or brain (legend to Fig. 2). After incubation for 48 to 72 hours, the oocytes were tested for $I_{Cl(Ca)}$ and I_{Ba} by voltage clamping. In oocytes injected with RNA from brain, skeletal muscle, and heart but not from liver, $I_{Cl(Ca)}$ was significantly increased, reaching amplitudes up to 2 μA. In addition, many oocytes injected with brain or heart RNA showed $I_{Cl(Ca)}$ with two peaks (Fig. 2A). In contrast to uninjected cells, injected cells displayed only partial (40 to 60 percent) inactivation of $I_{Cl(Ca)}$ when the membrane was depolarized from holding potentials more positive than −40 mV. Clearly, the injection of RNA isolated from excitable tissues altered several properties of $I_{Cl(Ca)}$.

In Cl^--free solution with high concentration of Ba^{2+}, large (up to 150 nA) voltage-sensitive inward currents were detected in oocytes injected with brain, skeletal muscle, or heart RNA. These currents were unchanged by addition of tetrodotoxin (1

N. Dascal, T. P. Snutch, and H. A. Lester, Division of Biology, California Institute of Technology, Pasadena 91125.
T. P. Snutch, H. Lübbert, and N. Davidson, Division of Chemistry and Chemical Engineering, California Institute of Technology, Pasadena 91125.

*To whom correspondence should be addressed.